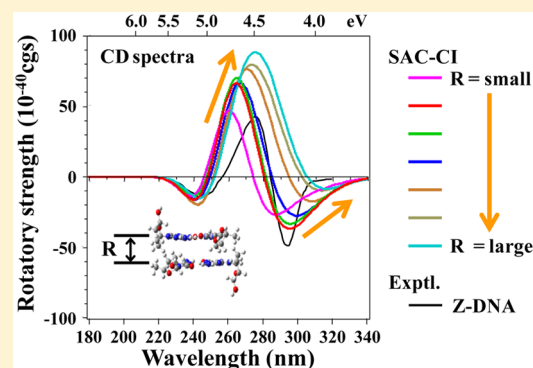


Indicator of the Stacking Interaction in the DNA Double-Helical Structure: ChiraSac Study

Tomoo Miyahara[†] and Hiroshi Nakatsuji^{*,†}[†]Quantum Chemistry Research Institute, Kyodai Katsura Venture Plaza, North building 107, 1-36 Goryo-Oohara, Nishikyō-ku, Kyoto, 615-8245, Japan**S** Supporting Information

ABSTRACT: The double-helical structures of DNA are experimentally distinguished by the circular dichroism (CD) spectra. The CD spectra are quite different between the left- and right-handed double-helical structures of DNA. The lowest peak is negative for the left-handed Z-DNA but positive for the right-handed B-DNA. Using the Z-DNA model with a strong stacking interaction, we examined whether the CD spectra depend on the distance between the two base pairs, deoxy-guanosine (dG) and deoxy-cytidine (dC). The result showed that the feature of the SAC-CI CD spectra changes from Z-DNA to B-DNA when increasing the distance between the two base pairs. Therefore, we concluded that the stacking interaction is the origin of the lowest negative peak, being the feature of the CD spectra of Z-DNA, and at the same time that the lack of the negative peak at about 290–300 nm of the CD spectra of B-DNA is due to the weak stacking interaction in B-DNA.



1. INTRODUCTION

In experiments, the transition between B- and Z-DNA is induced by the change in the temperature or salt concentration.^{1–8} At low temperature or in high-salt concentration, Z-DNA is the stable and preferred conformation. The B-Z transitions largely change the sign and shape of the electronic circular dichroism (CD) spectra^{2–8} and the vibrational circular dichroism (VCD) spectra.^{9–11} (In this article, the “CD” represents the electronic circular dichroism.) The feature is that the sign at 295 nm in the CD spectra is negative for the left-handed Z-DNA but positive for the right-handed B-DNA. We have already studied the CD spectra of B- and Z-DNA theoretically and have suggested that the negative peak at 295 nm in the CD spectra of Z-DNA is due to the stacking interaction between the two base pairs, deoxyguanosine (dG) and deoxycytidine (dC).¹² The stacking interaction contributes to the stability of the double-helical DNA's structures along with the hydrogen-bonding interaction. Therefore, Hobza and colleagues has made a detailed study of the stacking interaction.^{13–15} In the present article, we examined the CD spectra for the different distance between the two base pairs to clarify the relationship between the stacking interaction and the CD spectra of Z-DNA.

In general, the CD spectra depend largely on the conformation of the chiral molecule as well as the solvent and protein environment of the target molecule.⁸ Therefore, the CD spectra include the information on the target molecules as well as the surrounding environments. However, to obtain a lot of information from the CD spectra we need a highly reliable theory.

The SAC/SAC-CI method is a well-established theory for the ground and excited states^{16–19} and has been applied to many systems.^{20–24} Recently, we showed that the SAC/SAC-CI method is useful to analyze the CD spectra of DNA.¹² Therefore, we are constructing the ChiraSac,^{25,26} which is a new molecular technology for the CD spectra of chiral molecular systems using the SAC-CI and other useful methods on the Gaussian suite of programs.²⁷

Recently, the time-dependent density functional theory (TDDFT) using PBE0 functional showed reasonable agreement with the SAC-CI calculations in both transition energies and excited-state equilibrium structures.^{28,29} However, the accuracy is much different between the valence and Rydberg excited states and largely dependent on the functional.³⁰ Therefore, it is difficult to believe the Td-DFT results applied to the unknown molecular systems other than the molecules used for the determination of the functional parameters.

In the CD spectra of the double-helical structures of DNA, the negative peak at 295 nm was observed not for the right-handed B-DNA but for the left-handed Z-DNA.^{2–8} Our previous theoretical studies¹² also showed that the negative peak at 295 nm was calculated in the SAC-CI CD spectrum of Z-DNA in which the base pair stacks strongly with only one neighboring base pair. However, for B-DNA in which the base pair stacks weakly with both of the neighboring base pairs, the sign of the SAC-CI CD spectrum at 295 nm is positive.

Received: March 24, 2015

Revised: July 1, 2015

Published: July 2, 2015

Therefore, if the strong stacking interaction is the origin of the strong negative peak at 295 nm of Z-DNA, the CD spectra must be correlated to the distance between the two base pairs. Therefore, to elucidate the relationship between the CD spectra and the stacking interaction, we calculated the SAC-CI CD spectra of Z-DNA with changing the distance between the two base pairs using the program system ChiraSac. We also analyzed the absorption (UV) spectra as well as the CD spectra.

2. MODELING AND COMPUTATIONAL DETAILS

The geometries of Z-DNA were taken from the X-ray crystallography structure (PDB ID: 1DCG), which is arranged alternately with dG and dC (Figure 1a,b). Because the guanine-

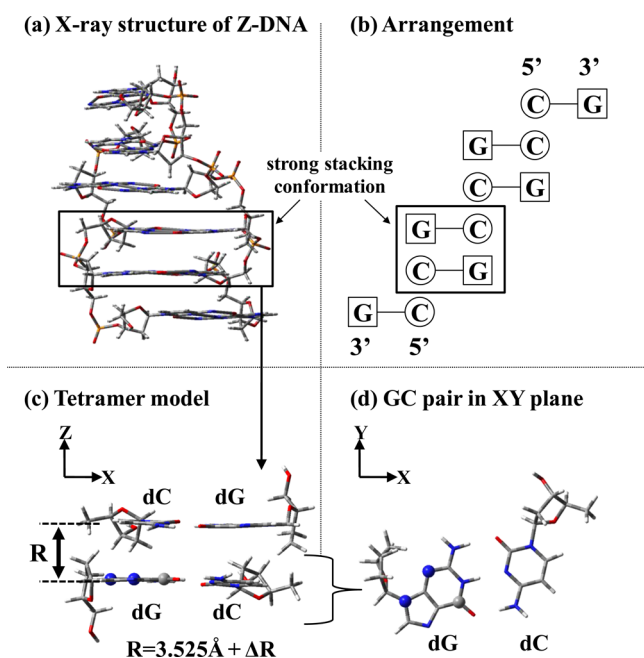


Figure 1. (a) X-ray crystallography structure of Z-DNA (PDB ID: 1DCG). (b) Arrangement of cytosine (C) and guanine (G). (c) Geometry of tetramer model. R represents the distance between the two base pairs. R is 3.525 Å for X-ray crystallography structure. (d) Geometry of one GC (dG and dC) pair. Three atoms indicated by "Ball" are arranged in the XY plane.

cytosine (GC) pair strongly stacks with another CG pair, we used the strongly stacked tetramer model, which is the same as the previous study of DNA¹² (Figure 1 c). We removed the phosphate group from the tetramer model to facilitate the elongation and the contraction of the distance R between the two base pairs. Three atoms indicated by "Ball" define the XY plane of one GC pair (Figure 1 d) and the interplanar distance R was changed. The coordinate of the tetramer model of the X-ray crystallography structure is shown in Supporting Information Table S1. Other models were formed by changing the Z-coordinate of the atoms numbered from 32 to 90 (see Supporting Information Table S1).

The average distance R between the two GC pairs is 3.525 Å for Z-DNA. We changed the distance R in the range of 3.525 – 0.2 to 3.525 + 2.0 Å. Although the GC pair rotates with the change of the distance R , we ignored the rotation of the GC pair and used the same arrangement. However, it is also interesting to examine the CD spectral change along with the rotation of the GC pair. We therefore calculated the rotational

models at the distance $R = 3.525$ and $3.525 + 2.0$ Å in which one GC pair rotates in a counterclockwise direction by 30° with respect to the other GC pair while other geometrical parameters are fixed (see Supporting Information Table S2). In the actual DNA, this rotation cannot occur at the distance of $R = 3.525$ Å due to the existence of the phosphate group.

For the SAC/SAC-CI calculations, the basis functions employed were D95(d)³¹ for nucleic acid bases and D95³¹ for deoxyribose of DNA, the core orbitals of the C, O, and N atoms were treated as frozen orbitals, and all single and selected double excitation operators were included. Perturbation selection³² was carried out with the threshold sets of 1×10^{-6} and 1×10^{-7} hartree for the SAC and SAC-CI calculations, respectively. The orbitals, whose energies were within -1.20 to $+1.20$ au, were chosen as the active orbitals. The SAC-CI CD spectra were convoluted using Gaussian envelopes to describe the Franck–Condon widths and the resolution of the spectrometer. The full width at half-maximum (fwhm) of the Gaussian envelope was 0.6 eV for the SAC-CI CD spectra and 0.4 eV for the SAC-CI UV spectra. The rotatory strengths (R_{0a}) of the CD spectra were calculated using the gauge-invariant velocity form given by the following equation

$$R_{0a} = \text{Im} \left\{ \frac{\langle \Psi_0 | \nabla | \Psi_a \rangle \langle \Psi_a | \hat{m} | \Psi_0 \rangle}{E_a - E_0} \right\} \quad (1)$$

3. SAC-CI CD SPECTRA

Figure 2 shows the SAC-CI CD spectra for the different distances R between the two GC pairs compared with the experimental CD spectra of Z- and B-DNA.² (The experimental CD spectrum of B-DNA is posted for comparison with the SAC-CI CD spectrum of the weakly stacked Z-DNA.) In order

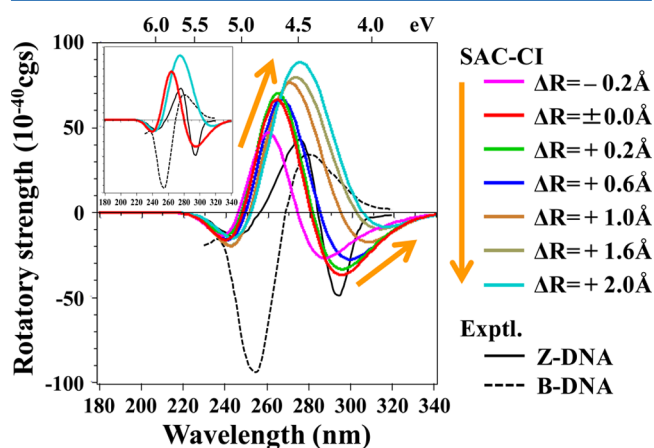


Figure 2. SAC-CI CD spectra (colored lines) for the different distance R between the two base pairs using the tetramer models of Z-DNA as compared with the experimental CD spectra of Z- and B-DNA (black lines).² All excited states of the SAC-CI calculation have been shifted to the lower values by 0.5 eV. The magenta, red, green, blue, gold, khaki, and cyan lines represent the SAC-CI CD spectra with $\Delta R = -0.2, \pm 0.0, +0.2, +0.6, +1.0, +1.6,$ and $+2.0$ Å. The black solid and dotted lines represent the experimental CD spectra of Z- and B-DNA, respectively. The orange arrows represent the direction of the SAC-CI CD spectral change in the increase of the distance R . The inset shows the two representative SAC-CI spectra with $\Delta R = \pm 0.0$ Å and $\Delta R = +2.0$ Å compared with the experimental CD spectra of Z- and B-DNA.

Table 1. Excited States of X-ray Model ($\Delta R = \pm 0.0 \text{ \AA}$)

state	SAC-CI						exptl. (eV/nm)	
	EE (eV) ^a	EE (nm) ^a	Osc ^b	Rot ^c	nature ^d	type ^e	CD ^f	UV ^f
1 ¹ A	4.60	270	0.003	-16.91	$\pi_{g,h} \rightarrow \pi_{c,l}^*$	ET(s)	4.19/296	
2 ¹ A	4.69	264	0.005	-5.72	$\pi_{g,h} \rightarrow \pi_{c,l}^*$	ET(s)	4.19/296	
3 ¹ A	4.88	254	0.010	-45.70	$\pi_{g,h} \rightarrow \pi_{g,l}^*$	dG	4.19/296	
4 ¹ A	4.92	252	0.191	72.61	$\pi_{c,h} \rightarrow \pi_{c,l}^*$	dC		4.28/290
5 ¹ A	4.93	252	0.053	-129.87	$\pi_{c,h} \rightarrow \pi_{c,l}^* + \pi_{c,h-1} \rightarrow \pi_{c,l}^*$	dC		4.28/290
6 ¹ A	4.99	248	0.053	12.25	$\pi_{g,h} \rightarrow \pi_{g,l}^* + \pi_{c,h-1} \rightarrow \pi_{c,l}^*$	dG + dC		4.28/290
7 ¹ A	5.06	245	0.014	35.45	$\pi_{c,h-1} \rightarrow \pi_{c,l}^* + \pi_{c,h} \rightarrow \pi_{c,l}^*$	dC		
8 ¹ A	5.16	240	0.541	121.83	$\pi_{c,h-1} \rightarrow \pi_{c,l}^*$	dC	4.51/275	4.84/256
9 ¹ A	5.27	235	0.034	-54.55	$n_g \rightarrow \pi_{g,l}^*$	dG		
10 ¹ A	5.29	234	0.415	138.46	$\pi_{g,h} \rightarrow \pi_{g,l+1}^*$	dG	4.51/275	4.84/256
11 ¹ A	5.35	232	0.303	-109.38	$\pi_{g,h} \rightarrow \pi_{g,l+1}^*$	dG		4.84/256
12 ¹ A	5.43	228	0.004	-5.28	$n_c \rightarrow \pi_{c,l}^*$	dC		
13 ¹ A	5.48	226	0.003	-7.85	$n_c \rightarrow \pi_{c,l}^*$	dC		
14 ¹ A	5.52	225	0.005	-6.09	$n_g \rightarrow \pi_{g,l+1}^*$	dG		

^aExcitation energy. ^bOscillator strength. ^cRotatory strength (10^{-40} cgs). ^dSubscript g and c represent guanine and cytosine, respectively. Subscript h, h-1, l and l+1 represent the highest occupied molecular orbital (HOMO), HOMO-1, the lowest unoccupied molecular orbital (LUMO) and LUMO+1 of dG or dC. ^edG and dC represent the intramolecular excited states of deoxyguanosine and deoxycytidine, respectively. ET(s) represents the electron transfer excited states from guanine to cytosine through the stacking interaction. ^fExperimental values of Z-DNA.²

Table 2. Excited States of $\Delta R = -0.2 \text{ \AA}$ Model

state	SAC-CI						exptl.(eV/nm)	
	EE (eV) ^a	EE (nm) ^a	Osc ^b	Rot ^c	nature ^d	type ^e	CD ^f	UV ^f
1 ¹ A	4.60	269	0.025	-71.29	$\pi_{g,h} \rightarrow \pi_{c,l}^*$	ET(s)	4.19/296	
2 ¹ A	4.61	269	0.001	54.27	$\pi_{g,h} \rightarrow \pi_{c,l}^*$	ET(s)		
3 ¹ A	4.83	256	0.145	61.62	$\pi_{c,h} \rightarrow \pi_{c,l}^*$	dC		4.28/290
4 ¹ A	4.91	252	0.080	-63.14	$\pi_{c,h} \rightarrow \pi_{c,l}^*$	dC		4.28/290
5 ¹ A	4.97	249	0.074	-72.52	$\pi_{g,h} \rightarrow \pi_{g,l}^*$	dG		4.28/290
6 ¹ A	5.04	246	0.003	-44.62	$\pi_{c,h-1} \rightarrow \pi_{c,l}^*$	dC		
7 ¹ A	5.09	244	0.012	38.41	$\pi_{g,h} \rightarrow \pi_{g,l}^* + \pi_{c,h-1} \rightarrow \pi_{c,l}^*$	dG + dC		
8 ¹ A	5.21	238	0.504	138.89	$\pi_{g,h} \rightarrow \pi_{g,l}^*$	dG	4.51/275	4.84/256
9 ¹ A	5.25	236	0.014	-39.52	$n_g \rightarrow \pi_{g,l}^*$	dG		
10 ¹ A	5.30	234	0.447	129.45	$\pi_{g,h} \rightarrow \pi_{g,l+1}^*$	dG	4.51/275	4.84/256
11 ¹ A	5.37	231	0.293	-119.97	$\pi_{g,h} \rightarrow \pi_{g,l+1}^*$	dG		4.84/256
12 ¹ A	5.42	229	0.004	-5.99	$n_c \rightarrow \pi_{c,l}^*$	dC		
13 ¹ A	5.49	226	0.003	-7.06	$n_c \rightarrow \pi_{c,l}^*$	dC		
14 ¹ A	5.53	224	0.004	-6.97	$n_g \rightarrow \pi_{g,l}^*$	dG		

^aExcitation energy. ^bOscillator strength. ^cRotatory strength (10^{-40} cgs). ^dSubscript g and c represent guanine and cytosine, respectively. Subscript h,h-1,l and l+1 represent the highest occupied molecular orbital (HOMO), HOMO-1, the lowest unoccupied molecular orbital (LUMO) and LUMO+1 of dG or dC. ^edG and dC represent the intramolecular excited states of deoxyguanosine and deoxycytidine, respectively. ET(s) represents the electron transfer excited states from guanine to cytosine through the stacking interaction. ^fExperimental values of Z-DNA.²

to compare with the experimental spectra, the SAC-CI results have been shifted to the lower energy by 0.5 eV, because we cut the active space as explained in the previous section. The natures of the excited states are shown in Tables 1–7: Table 1 for $\Delta R = \pm 0.0 \text{ \AA}$, Table 2 for $\Delta R = -0.2 \text{ \AA}$, Table 3 for $\Delta R = +0.2 \text{ \AA}$, Table 4 for $\Delta R = +0.6 \text{ \AA}$, Table 5 for $\Delta R = +1.0 \text{ \AA}$, Table 6 for $\Delta R = +1.6 \text{ \AA}$, and Table 7 for $\Delta R = +2.0 \text{ \AA}$. We will discuss the natures of the excited states in some details in Section 5.

We used the distance ($R = 3.525 \text{ \AA}$, $\Delta R = \pm 0.0 \text{ \AA}$) taken from the X-ray structural data of Z-DNA as a standard distance and calculated the CD spectra at different ΔR ($= -0.2$ to $+2.0 \text{ \AA}$). As ΔR increases, the intensity of the negative peak at 295 nm becomes weak. Also, the intensity at 295 nm is weaker for $\Delta R = -0.2 \text{ \AA}$ than for $\Delta R = \pm 0.0 \text{ \AA}$. When the tetramer model is the X-ray structure ($\Delta R = \pm 0.0 \text{ \AA}$), the peak at 295 nm has the strongest negative intensity. In addition, as the distance ΔR

becomes large (the stacking interaction between the two GC pairs becomes weak), the SAC-CI CD spectra come close to the experimental CD spectrum of B-DNA from that of Z-DNA. Therefore, the stacking interaction between the two GC pairs is strong for Z-DNA but weak for B-DNA.

The lowest excited state of the X-ray model ($\Delta R = \pm 0.0 \text{ \AA}$) is the electron transfer (ET) excited states from guanine to cytosine. The ET occurs through the stacking interaction, not the hydrogen-bonding interaction. However, as ΔR increases, the excitation energy of the ET excited state becomes higher than that of the X-ray model. Therefore, these results indicate that the negative peak at 295 nm is the indicator of the stacking interaction between the two base pairs of DNA.

4. SAC-CI UV SPECTRA

Figure 3 shows the SAC-CI UV spectra for the different distance R between the two GC pairs compared with the

Table 3. Excited States of $\Delta R = +0.2 \text{ \AA}$ Model

state	SAC-CI					exptl.(eV/nm)		
	EE (eV) ^a	EE (nm) ^a	Osc ^b	Rot ^c	nature ^d	type ^e	CD ^f	UV ^f
1 ¹ A	4.57	271	0.005	-13.25	$\pi_{g,h} \rightarrow \pi_{c,l}^*$	ET(s)	4.19/296	
2 ¹ A	4.71	263	0.013	-47.53	$\pi_{g,h} \rightarrow \pi_{c,l}^*$	ET(s)	4.19/296	
3 ¹ A	4.76	261	0.126	80.35	$\pi_{c,h} \rightarrow \pi_{c,l}^*$	dC		4.28/290
4 ¹ A	4.86	255	0.070	-93.75	$\pi_{g,h} \rightarrow \pi_{g,l}^*$	dG		4.28/290
5 ¹ A	4.94	251	0.019	-15.78	$\pi_{g,h} \rightarrow \pi_{g,l}^* + \pi_{c,h-1} \rightarrow \pi_{c,l}^*$	dG + dC		
6 ¹ A	4.97	249	0.058	-98.80	$\pi_{c,h-1} \rightarrow \pi_{c,l}^*$	dC		
7 ¹ A	5.05	246	0.027	157.79	$\pi_{c,h-1} \rightarrow \pi_{c,l}^* + \pi_{c,h} \rightarrow \pi_{c,l}^*$	dC	4.51/275	
8 ¹ A	5.15	241	0.556	63.53	$\pi_{c,h} \rightarrow \pi_{c,l}^*$	dC	4.51/275	4.84/256
9 ¹ A	5.29	234	0.464	69.59	$\pi_{g,h} \rightarrow \pi_{g,l+1}^*$	dG	4.51/275	4.84/256
10 ¹ A	5.31	233	0.004	15.15	$n_g \rightarrow \pi_{g,l}^*$	dG		
11 ¹ A	5.35	232	0.301	-91.29	$\pi_{g,h} \rightarrow \pi_{g,l+1}^*$	dG		4.84/256
12 ¹ A	5.42	229	0.003	-4.87	$n_c \rightarrow \pi_{c,l}^*$	dC		
13 ¹ A	5.46	227	0.003	-5.50	$n_c \rightarrow \pi_{c,l}^*$	dC		
14 ¹ A	5.52	225	0.004	-5.96	$n_g \rightarrow \pi_{g,l+1}^*$	dG		

^aExcitation energy. ^bOscillator strength. ^cRotatory strength (10^{-40} cgs). ^dSubscript g and c represent guanine and cytosine, respectively. Subscript h, h-1, l and l+1 represent the highest occupied molecular orbital (HOMO), HOMO-1, the lowest unoccupied molecular orbital (LUMO) and LUMO+1 of dG or dC. ^edG and dC represent the intramolecular excited states of deoxyguanosine and deoxycytidine, respectively. ET(s) represents the electron transfer excited states from guanine to cytosine through the stacking interaction. ^fExperimental values of Z-DNA.²

Table 4. Excited States of $\Delta R = +0.6 \text{ \AA}$ Model

state	SAC-CI					exptl. (eV/nm)		
	EE (eV) ^a	EE (nm) ^a	Osc ^b	Rot ^c	nature ^d	type ^e	CD ^f	UV ^f
1 ¹ A	4.68	265	0.085	-58.33	$\pi_{c,h} \rightarrow \pi_{c,l}^*$	dC	4.19/296	4.28/290
2 ¹ A	4.78	260	0.124	103.97	$\pi_{g,h} \rightarrow \pi_{g,l}^*$	dG		4.28/290
3 ¹ A	4.80	258	0.008	-73.96	$\pi_{g,h} \rightarrow \pi_{c,l}^* + \pi_{g,h} \rightarrow \pi_{g,l}^*$	ET(s)+dG	4.19/296	
4 ¹ A	4.87	255	0.077	-33.03	$\pi_{c,h} \rightarrow \pi_{c,l}^* + \pi_{c,h-1} \rightarrow \pi_{c,l}^*$	dC		
5 ¹ A	4.88	254	0.036	-12.80	$\pi_{g,h} \rightarrow \pi_{c,l}^*$	ET(s)		
6 ¹ A	4.92	252	0.024	5.10	$\pi_{g,h} \rightarrow \pi_{c,l}^*$	ET(s)		
7 ¹ A	5.01	247	0.021	-42.42	$\pi_{c,h-1} \rightarrow \pi_{c,l}^*$	dC		
8 ¹ A	5.09	243	0.495	148.34	$\pi_{c,h-1} \rightarrow \pi_{c,l}^*$	dC	4.51/275	4.84/256
9 ¹ A	5.27	235	0.431	53.16	$\pi_{g,h} \rightarrow \pi_{g,l+1}^*$	dG	4.51/275	4.84/256
10 ¹ A	5.35	232	0.006	10.41	$n_g \rightarrow \pi_{g,l}^*$	dG		
11 ¹ A	5.37	231	0.367	-72.60	$\pi_{g,h} \rightarrow \pi_{g,l+1}^*$	dG		4.84/256
12 ¹ A	5.42	229	0.004	-4.73	$n_c \rightarrow \pi_{c,l}^*$	dC		
13 ¹ A	5.45	227	0.002	-5.49	$n_c \rightarrow \pi_{c,l}^*$	dC		
14 ¹ A	5.49	226	0.003	-2.75	$n_g \rightarrow \pi_{g,l+1}^*$	dG		

^aExcitation energy. ^bOscillator strength. ^cRotatory strength (10^{-40} cgs). ^dSubscript g and c represent guanine and cytosine, respectively. Subscript h, h-1, l and l+1 represent the highest occupied molecular orbital (HOMO), HOMO-1, the lowest unoccupied molecular orbital (LUMO) and LUMO+1 of dG or dC. ^edG and dC represent the intramolecular excited states of deoxyguanosine and deoxycytidine, respectively. ET(s) represents the electron transfer excited states from guanine to cytosine through the stacking interaction. ^fExperimental values of Z-DNA.²

experimental UV spectra of Z- and B-DNA.² (The experimental UV spectrum of B-DNA is posted for comparison with the SAC-CI UV spectrum of the weakly stacked Z-DNA.) In order to compare with the experimental spectra, the SAC-CI results have been shifted to the lower energy by 0.5 eV likewise in the SAC-CI CD spectra. The inset shows the representative SAC-CI results corresponding to the structures of Z-DNA ($\Delta R = \pm 0.0 \text{ \AA}$) and $\Delta R = +2.0 \text{ \AA}$. The natures of the excited states are shown in Tables 1 to 7, similarly to the CD cases given above. We will discuss the natures of the excited states in some details in Section 5.

The change in the SAC-CI UV spectra was small compared to that of the CD spectra. So, we cannot assign the Z- and B-DNA from the UV spectra alone. However, in close examination we see that the intensity of the SAC-CI UV spectra is slightly different for both main and shoulder peaks. As will be clarified later in the next section, we see from Tables 1

and 7 that the shoulder peak at 290 nm corresponds to the ET excited states for the X-ray model ($\Delta R = \pm 0.0 \text{ \AA}$) with the strong stacking interaction but to the intramolecular excited states for the $\Delta R = +2.0 \text{ \AA}$ model with the weak stacking interaction. Therefore, the oscillator strength is weak for the strong stacking models, but is strong for the weak stacking models, though the shoulder peak is stronger for Z-DNA than for B-DNA. For the main peak, the excitation energy changes little among all models, and the oscillator strength is strong for $\Delta R = \pm 0.0$ and $+2.0 \text{ \AA}$ but is weak for $+0.6$ and $+1.0 \text{ \AA}$. Both main and shoulder peaks of the UV spectra seem not to be correlated to the stacking interaction.

5. EXCITED STATES

The excitation energies, oscillator strengths, rotatory strengths, natures, and type of the excited states obtained from the SAC-CI calculations for $\Delta R = \pm 0.0, -0.2, +0.2, +0.6, +1.0, +1.6,$ and

Table 5. Excited States of $\Delta R = +1.0 \text{ \AA}$ Model

state	SAC-CI						exptl.(eV/nm)	
	EE (eV) ^a	EE (nm) ^a	Osc ^b	Rot ^c	nature ^d	type ^e	CD ^f	UV ^f
1 ¹ A	4.70	264	0.039	-83.77	$\pi_{c,h} \rightarrow \pi_{c,l}^*$	dC	4.19/296	
2 ¹ A	4.76	260	0.089	-98.98	$\pi_{g,h} \rightarrow \pi_{g,l}^*$	dG	4.19/296	4.28/290
3 ¹ A	4.80	258	0.107	208.94	$\pi_{c,h} \rightarrow \pi_{c,l}^* + \pi_{g,h} \rightarrow \pi_{c,l}^*$	dC + ET(s)	4.43/280 (B-DNA)	4.28/290
4 ¹ A	4.86	255	0.021	0.34	$\pi_{g,h} \rightarrow \pi_{c,l}^*$	ET(s)		
5 ¹ A	4.88	254	0.075	-13.86	$\pi_{c,h} \rightarrow \pi_{c,l}^*$	dC		
6 ¹ A	4.89	254	0.058	-23.30	$\pi_{g,h} \rightarrow \pi_{c,l}^*$	ET(s)		
7 ¹ A	5.03	247	0.083	-20.51	$\pi_{c,h-1} \rightarrow \pi_{c,l}^*$	dC		
8 ¹ A	5.10	243	0.090	-17.33	$\pi_{g,h} \rightarrow \pi_{c,l}^*$	ET(h)		
9 ¹ A	5.12	242	0.344	124.58	$\pi_{c,h-1} \rightarrow \pi_{c,l}^*$	dC	4.51/275	4.84/256
10 ¹ A	5.23	237	0.413	39.08	$\pi_{g,h} \rightarrow \pi_{g,l+1}^*$	dG		4.84/256
11 ¹ A	5.34	232	0.013	15.77	$n_g \rightarrow \pi_{g,l}^*$	dG		
12 ¹ A	5.37	231	0.376	-74.07	$\pi_{g,h} \rightarrow \pi_{g,l+1}^*$	dG		4.84/256
13 ¹ A	5.46	227	0.004	-7.22	$n_c \rightarrow \pi_{c,l}^*$	dC		
14 ¹ A	5.48	226	0.002	-3.77	$n_g \rightarrow \pi_{g,l+1}^*$	dG		

^aExcitation energy. ^bOscillator strength. ^cRotatory strength (10^{-40} cgs). ^dSubscript g and c represent guanine and cytosine, respectively. Subscript h, h-1, l and l+1 represent the highest occupied molecular orbital (HOMO), HOMO-1, the lowest unoccupied molecular orbital (LUMO) and LUMO+1 of dG or dC. ^edG and dC represent the intramolecular excited states of deoxyguanosine and deoxycytidine, respectively. ET(s) and ET(h) represent the electron transfer excited states from guanine to cytosine through the stacking and hydrogen-bonding interactions, respectively. ^fExperimental values of Z-DNA except for "B-DNA".²

Table 6. Excited states of $\Delta R = +1.6 \text{ \AA}$ model

state	SAC-CI						exptl.(eV/nm)	
	EE (eV) ^a	EE (nm) ^a	Osc ^b	Rot ^c	nature ^d	type ^e	CD ^f	UV ^f
1 ¹ A	4.69	264	0.052	-80.84	$\pi_{c,h} \rightarrow \pi_{c,l}^*$	dC	4.19/296	
2 ¹ A	4.73	262	0.129	-31.58	$\pi_{g,h} \rightarrow \pi_{g,l}^*$	dG	4.19/296	4.28/290
3 ¹ A	4.82	257	0.118	191.86	$\pi_{c,h} \rightarrow \pi_{c,l}^*$	dC	4.43/280 (B-DNA)	4.28/290
4 ¹ A	4.89	254	0.141	-64.90	$\pi_{c,h} \rightarrow \pi_{c,l}^*$	dC		4.28/290
5 ¹ A	4.98	249	0.002	5.12	$\pi_{g,h} \rightarrow \pi_{c,l}^*$	ET(s)		
6 ¹ A	5.01	247	0.001	8.26	$\pi_{g,h} \rightarrow \pi_{c,l}^*$	ET(h)		
7 ¹ A	5.06	245	0.038	1.04	$\pi_{g,h} \rightarrow \pi_{c,l}^*$	ET(s)		
8 ¹ A	5.08	244	0.200	8.50	$\pi_{c,h-1} \rightarrow \pi_{c,l}^*$	dC		4.84/256
9 ¹ A	5.20	239	0.468	59.78	$\pi_{g,h} \rightarrow \pi_{g,l+1}^*$	dG	4.51/275	4.84/256
10 ¹ A	5.23	237	0.184	59.20	$\pi_{c,h-1} \rightarrow \pi_{c,l}^*$	dC	4.51/275	4.84/256
11 ¹ A	5.35	232	0.240	2.48	$\pi_{g,h} \rightarrow \pi_{g,l+1}^* + n_g \rightarrow \pi_{g,l}^*$	dG		4.84/256
12 ¹ A	5.36	231	0.170	-83.06	$n_g \rightarrow \pi_{g,l}^*$	dG		4.84/256
13 ¹ A	5.52	225	0.002	-4.49	$n_g \rightarrow \pi_{g,l+1}^*$	dG		
14 ¹ A	5.55	224	0.002	-2.36	$\pi_{g,h} \rightarrow \pi_{c,l}^* + n_c \rightarrow \pi_{c,l}^*$	ET(h) + dC		

^aExcitation energy. ^bOscillator strength. ^cRotatory strength (10^{-40} cgs). ^dSubscript g and c represent guanine and cytosine, respectively. Subscript h, h-1, l and l+1 represent the highest occupied molecular orbital (HOMO), HOMO-1, the lowest unoccupied molecular orbital (LUMO) and LUMO+1 of dG or dC. ^edG and dC represent the intramolecular excited states of deoxyguanosine and deoxycytidine, respectively. ET(s) and ET(h) represent the electron transfer excited states from guanine to cytosine through the stacking and hydrogen-bonding interactions, respectively. ^fExperimental values of Z-DNA except for "B-DNA".²

+2.0 \AA models are shown in Table 1–7. Because each model includes two guanine and two cytosine, each model has two orbitals corresponding to the monomer orbital of guanine or cytosine. These tables will clarify in more details the origins of the behaviors in the CD spectra for different R of the present Z-DNA.

(1) **Table 1 for the X-ray model ($\Delta R = \pm 0.0 \text{ \AA}$).** The lowest two excited states are the electron transfer (ET) excitation from guanine to cytosine through the stacking interaction and their rotatory strengths have a negative sign. The 3¹A excited state is the intramolecular excitation of guanine and its rotatory strength is also strong negative. Therefore, the lowest three excited states are the origin of the negative peak at 295 nm of CD spectra of Z-DNA. The origin of the positive peak at 275 nm is the 8 and 10¹A excited states with a strong

positive rotatory strength. The 8 and 10¹A excited states are the intramolecular excitation of cytosine and guanine, respectively.

For the experimental UV spectrum of Z-DNA, the 4, 5, and 6¹A excited states that have the considerable oscillator strengths are the origin of the shoulder peak at 290 nm and the 8, 10 and 11¹A excited states are the origin of the main peak at 256 nm. The six excited states have the strong oscillator strength due to the intramolecular excitation of guanine or cytosine.

(2) **Table 2 for $\Delta R = -0.2 \text{ \AA}$ model.** The lowest two excited states are the ET excitation through the stacking interaction. The 3¹A excited state is the intramolecular excitation, corresponding to the 4¹A excited state of the X-ray model. Because the rotatory strength is negative for 1¹A excited state but positive for the 2 and 3¹A excited states, the intensity at 295 nm is weaker than that of the X-ray model. The intensity

Table 7. Excited States of $\Delta R = +2.0 \text{ \AA}$ Model

state	SAC-CI						exptl.(eV/nm)	
	EE(eV) ^a	EE(nm) ^a	Osc ^b	Rot ^c	nature ^d	type ^e	CD ^f	UV ^f
1 ¹ A	4.68	265	0.011	-99.36	$\pi_{c,h} \rightarrow \pi_{c,l}^* + \pi_{g,h} \rightarrow \pi_{g,l}^*$	dC + dG	4.19/296	
2 ¹ A	4.71	263	0.186	5.62	$\pi_{g,h} \rightarrow \pi_{g,l}^* + \pi_{c,h} \rightarrow \pi_{c,l}^*$	dG + dC		4.28/290
3 ¹ A	4.81	258	0.127	160.93	$\pi_{c,h} \rightarrow \pi_{c,l}^* + \pi_{g,h} \rightarrow \pi_{g,l}^*$	dC + dG	4.43/280 (B-DNA)	4.28/290
4 ¹ A	4.90	253	0.192	-39.39	$\pi_{c,h} \rightarrow \pi_{c,l}^*$	dC		4.28/290
5 ¹ A	5.05	246	0.030	3.12	$\pi_{g,h} \rightarrow \pi_{c,l}^*$	ET(h)		
6 ¹ A	5.08	244	0.002	2.99	$\pi_{g,h} \rightarrow \pi_{c,l}^*$	ET(s)		
7 ¹ A	5.15	241	0.061	203.00	$\pi_{g,h} \rightarrow \pi_{c,l}^* + \pi_{c,h-1} \rightarrow \pi_{c,l}^*$	ET(s) + dC	4.51/275	
8 ¹ A	5.17	240	0.069	137.68	$\pi_{c,h-1} \rightarrow \pi_{c,l}^* + \pi_{g,h} \rightarrow \pi_{c,l}^*$	dC + ET(s)	4.51/275	
9 ¹ A	5.18	239	0.464	-296.16	$\pi_{g,h} \rightarrow \pi_{g,l+1}^*$	dG		4.84/256
10 ¹ A	5.26	236	0.142	214.19	$\pi_{c,h-1} \rightarrow \pi_{c,l}^*$	dC		4.84/256
11 ¹ A	5.29	234	0.467	-199.79	$\pi_{g,h} \rightarrow \pi_{g,l+1}^*$	dG		4.84/256
12 ¹ A	5.38	231	0.001	-4.13	$n_g \rightarrow \pi_{g,l}^*$	dG		
13 ¹ A	5.46	227	0.006	3.05	$\pi_{g,h} \rightarrow \pi_{c,l}^*$	ET(h)		
14 ¹ A	5.55	223	0.001	-6.03	$n_g \rightarrow \pi_{g,l+1}^*$	dG		

^aExcitation energy. ^bOscillator strength. ^cRotatory strength (10^{-40} cgs). ^dSubscript g and c represent guanine and cytosine, respectively. Subscript h, h-1, l and l+1 represent the highest occupied molecular orbital (HOMO), HOMO-1, the lowest unoccupied molecular orbital (LUMO) and LUMO+1 of dG or dC. ^edG and dC represent the intramolecular excited states of deoxyguanosine and deoxycytidine, respectively. ET(s) and ET(h) represent the electron transfer excited states from guanine to cytosine through the stacking and hydrogen-bonding interactions, respectively. ^fExperimental values of Z-DNA except for "B-DNA".²

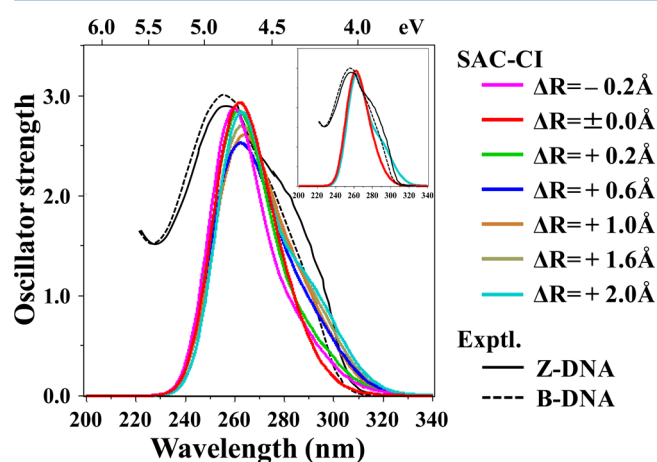


Figure 3. SAC-CI UV spectra (colored lines) for the different distance R between the two base pairs using the tetramer models of Z-DNA as compared with the experimental UV spectra of Z- and B-DNA (black lines).² All excited states of the SAC-CI calculations have been shifted to the lower values by 0.5 eV. The magenta, red, green, blue, gold, khaki, and cyan lines represent the SAC-CI UV spectra with $\Delta R = -0.2, \pm 0.0, +0.2, +0.6, +1.0, +1.6,$ and $+2.0 \text{ \AA}$. The black solid and dotted lines represent the experimental UV spectra of Z- and B-DNA, respectively. The inset shows the two representative SAC-CI spectra with $\Delta R = \pm 0.0 \text{ \AA}$ and $\Delta R = +2.0 \text{ \AA}$ compared with the experimental UV spectra of Z- and B-DNA.

at 275 nm is also weaker than that of the X-ray model due to the 4, 5, and 6¹A excited states with a negative rotatory strength. Although the distance change between the two base pairs has an effect on the excitation energies and the order of the excited states, the SAC-CI UV spectrum is little changed from the X-ray model.

(3) Table 3 for $\Delta R = +0.2 \text{ \AA}$ model. The SAC-CI CD spectrum is similar to that of the X-ray model. However, the order of the lowest two intramolecular excited states (3 and 4¹A) switches between the $\Delta R = \pm 0.0$ and $+0.2 \text{ \AA}$ models. Therefore, the intensity of the $\Delta R = +0.2 \text{ \AA}$ model is slightly weaker than that of the X-ray model. However, the features of

the excited states involved in the UV spectrum are almost the same as those of the $\Delta R = \pm 0.0$ and -0.2 \AA models.

(4) Table 4 for $\Delta R = +0.6 \text{ \AA}$ model. The lowest two excited states are the intramolecular excitation of cytosine or guanine. Because the distance between the two base pairs is longer than those of the strong stacking models ($\Delta R \leq +0.2 \text{ \AA}$), the ET excited states (3, 5, and 6¹A) are calculated to be at a higher energy region. Because the rotatory strength is strong negative for the 1 and 3¹A excited states but is strong positive for the 2¹A excited state, the negative peak at 295 nm is weak due to the cancellation. However, the excitation energies of the 8 and 9¹A excited states, assigned to the positive peak at 275 nm, are close to those of the $\Delta R = \pm 0.0$ and $+0.2 \text{ \AA}$ models. Therefore, the SAC-CI CD spectrum is similar to those of the $\Delta R = \pm 0.0$ and $+0.2 \text{ \AA}$ models.

For the SAC-CI UV spectrum, since the intramolecular excited states (1 and 2¹A) are calculated to be at a lower energy region, the shoulder peak at 290 nm is stronger than that of the strong stacking models ($\Delta R \leq +0.2 \text{ \AA}$). For the main peak, three excited states (8, 9, and 11¹A) are divided by 0.28 eV for the $\Delta R = +0.6 \text{ \AA}$ model but are within the range of 0.2 eV for the strong stacking models. Therefore, the main peak at 275 nm is weak and broad, as compared with the strong stacking models.

(5) Table 5 for $\Delta R = +1.0 \text{ \AA}$ model. The lowest two excited states are intramolecular excitation. The ET excited states (3, 4, and 6¹A) are calculated to be at a higher region. The rotatory strength is strong negative for the 1 and 2¹A excited states, but strong positive for the 3¹A excited state. Because the excitation energy gap between the 2 and 3¹A excited states is small, their rotatory strengths cancel. Therefore, the intensity at 295 nm is weaker than those of the $\Delta R \leq +0.6 \text{ \AA}$ models. The ET excited state through the hydrogen-bonding interaction is calculated to be at 5.10 eV (8¹A). Because five excited states (4, 5, 6, 7, and 8¹A), which lie between two excited states (3 and 9¹A) with a strong positive rotatory strength, have a weak rotatory strength, the 3¹A excited state contributes to the positive main peak. Therefore, the positive peak at 275 nm is calculated to be at a lower region

than those of the $\Delta R \leq +0.6 \text{ \AA}$ models. On the other hand, for the UV spectrum the feature of the excited states has the same feature as those of the $\Delta R = +0.6 \text{ \AA}$ model.

(6) **Table 6 for $\Delta R = +1.6 \text{ \AA}$ model.** The lowest four excited states are the intramolecular excitation. The negative rotatory strengths of the 1 and 2^1A excited states are canceled by the 3^1A excited state. The 3^1A excited state contributes to the positive peak in the same way as the $\Delta R = +1.0 \text{ \AA}$ model. The ET excited states (5, 6, and 7^1A) do not contribute to both CD and UV spectra due to the small oscillator and rotatory strengths.

The shoulder peak of the UV spectrum is slightly strong due to the lowest four excited states with the strong oscillator strength. For the main peak, the oscillator strength is strong due to five excited states (8, 9, 10, 11, and 12^1A), which is different from the $\Delta R \leq +1.0 \text{ \AA}$ models. However, the sum of oscillator strengths is almost the same as those of other models. As a result, both CD and UV spectra are similar to those of the $\Delta R = +1.0 \text{ \AA}$ model.

(7) **Table 7 for $\Delta R = +2.0 \text{ \AA}$ model.** The lowest four excited states are the intramolecular excitation. The hydrogen-bonding ET excited state (5^1A) is calculated to be lower than the stacking ET excited states (6, 7 and 8^1A). The intensity at 295 nm is weak due to the cancellation of the positive peak (3^1A), similar to the $\Delta R = +1.0$ and $+1.6 \text{ \AA}$ models. On the other hand, the intensity at 275 nm is stronger than those of the other models due to the 7 and 8^1A excited states with a strong positive rotatory strength. They are the intramolecular excitation of cytosine and the stacking ET excitation. In addition, the positive peak at 275 nm is red-shifted due to the 3^1A excited state with a strong positive rotatory strength. As a result, the SAC-CI CD spectrum of the $\Delta R = +2.0 \text{ \AA}$ model is similar to the experimental CD spectrum of B-DNA, whose stacking interaction is weak. However, the feature of the UV spectrum is the same as that of the $\Delta R = +0.6, +1.0$ and $+1.6 \text{ \AA}$ models, except that the intensity is slightly different.

6. ROTATIONAL EFFECT

We have revealed that the CD spectra of DNA strongly correlated to the distance between the two base pairs. However, in the actual DNA, as the distance between the two base pairs increases, one base pair rotates with respect to the other base pair. Therefore, we examine here the CD spectral change by the rotation of the base pair using the rotational models, in which one base pair rotates in a counterclockwise direction by 30° with respect to the other base pair for the $\Delta R = \pm 0.0$ and $+2.0 \text{ \AA}$ models. Figure 4a,b shows the top views of the normal and rotational models, respectively. In the normal model, the overlap between the two bases is small, because there is a carbon atom of the pyrimidine base in the center of the six-

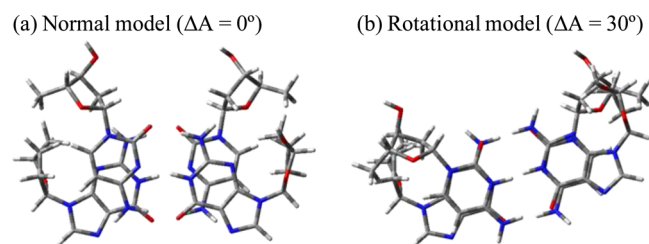


Figure 4. Top views of (a) the normal model and (b) the rotational model.

membered ring of the purine base. On the other hand, in the rotational model, the six-membered ring of the purine base tidily overlaps with the pyrimidine base. Actually, the rotation from the $\Delta R = \pm 0.0 \text{ \AA}$ model cannot occur due to the existence of the phosphate group. However, we can elucidate the rotational effect using the computational models.

Figures 5 and 6 show the SAC-CI CD and UV spectra for the normal and rotational models at the distance $\Delta R = \pm 0.0$ and

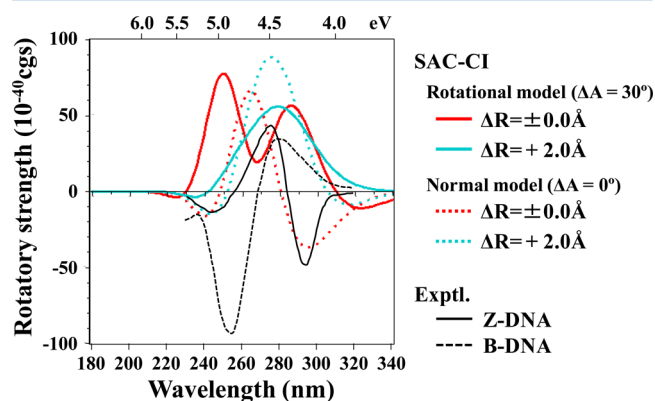


Figure 5. SAC-CI CD spectra (colored lines) for the different distance R and the different angle A between the two base pairs using the tetramer models of Z-DNA as compared with the experimental CD spectra of Z- and B-DNA (black lines).² All excited states of the SAC-CI calculation have been shifted to the lower values by 0.5 eV. The colored solid and dotted lines represent the SAC-CI CD spectra of the rotational ($\Delta A = 30^\circ$) and normal ($\Delta A = 0^\circ$) models, respectively. The red and cyan lines represent the SAC-CI CD spectra with $\Delta R = \pm 0.0$ and $+2.0 \text{ \AA}$, respectively. The black solid and dotted lines represent the experimental CD spectra of Z- and B-DNA, respectively.

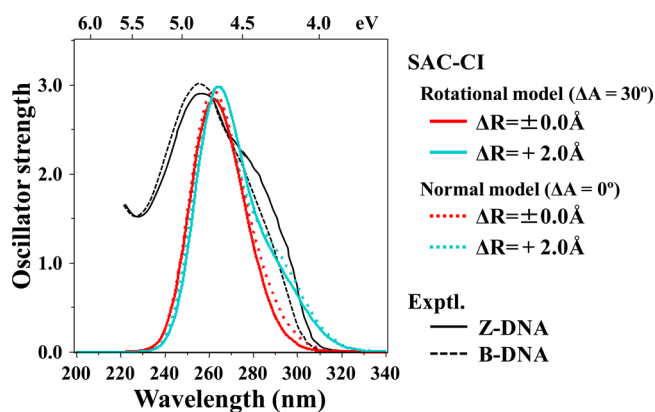


Figure 6. SAC-CI UV spectra (colored lines) for the different distance R and the different angle A between the two base pairs using the tetramer models of Z-DNA as compared with the experimental UV spectra of Z- and B-DNA (black lines).² All excited states of the SAC-CI calculations have been shifted to the lower values by 0.5 eV. The colored solid and dotted lines represent the SAC-CI UV spectra of the rotational ($\Delta A = 30^\circ$) and normal ($\Delta A = 0^\circ$) models, respectively. The red and cyan lines represent the SAC-CI UV spectra with $\Delta R = \pm 0.0$ and $+2.0 \text{ \AA}$, respectively. The black solid and dotted lines represent the experimental UV spectra of Z- and B-DNA, respectively.

$+2.0 \text{ \AA}$ compared with the experimental CD and UV spectra of Z- and B-DNA.² The “normal” model represents the X-ray or $\Delta R = +2.0 \text{ \AA}$ models. In order to compare with the experimental spectra, the SAC-CI results have been shifted to the lower energy by 0.5 eV, because we cut the active space as

Table 8. Excited States of the Rotational Model at $\Delta R = \pm 0.0$ ($\Delta A = 30^\circ$)

state	SAC-CI						Exptl.(eV/nm)	
	EE (eV) ^a	EE (nm) ^a	Osc ^b	Rot ^c	nature ^d	type ^e	CD ^f	UV ^f
1 ¹ A	4.46	278	0.001	-33.94	$\pi_{g,h} \rightarrow \pi_{c,l}^*$	ET(s)	4.19/296	4.28/290
2 ¹ A	4.55	272	0.001	10.50	$\pi_{g,h} \rightarrow \pi_{c,l}^*$	ET(s)		4.28/290
3 ¹ A	4.97	249	0.139	300.32	$\pi_{c,h} \rightarrow \pi_{c,l}^*$	dC	4.51/275	
4 ¹ A	5.02	247	0.155	-56.16	$\pi_{c,h-1} \rightarrow \pi_{c,l}^*$	dC		4.28/290
5 ¹ A	5.07	245	0.006	-3.24	$\pi_{c,h-1} \rightarrow \pi_{c,l}^*$	dC		
6 ¹ A	5.08	244	0.135	-181.94	$\pi_{g,h} \rightarrow \pi_{g,l}^*$	dG		4.28/290
7 ¹ A	5.21	238	0.422	-162.76	$\pi_{g,h} \rightarrow \pi_{g,l+1}^*$	dG		4.84/256
8 ¹ A	5.23	237	0.023	-130.88	$\pi_{c,h} \rightarrow \pi_{c,l}^* + \pi_{g,h} \rightarrow \pi_{g,l}^*$	dC + dG		
9 ¹ A	5.30	234	0.480	375.74	$\pi_{g,h} \rightarrow \pi_{g,l}^*$	dG	4.51/275	4.84/256
10 ¹ A	5.36	231	0.147	10.47	$\pi_{g,h} \rightarrow \pi_{g,l+1}^*$	dG		4.84/256
11 ¹ A	5.42	229	0.004	2.55	$n_g \rightarrow \pi_{g,l}^*$	dG		
12 ¹ A	5.60	222	0.005	-7.49	$n_g \rightarrow \pi_{c,l}^* + n_c \rightarrow \pi_{c,l}^*$	ET(h)+dC		
13 ¹ A	5.65	220	0.003	-7.03	$n_g \rightarrow \pi_{g,l}^*$	dG		
14 ¹ A	5.77	215	0.003	-6.27	$n_c \rightarrow \pi_{c,l}^*$	dC		

^aExcitation energy. ^bOscillator strength. ^cRotatory strength (10^{-40} cgs). ^dSubscript g and c represent guanine and cytosine, respectively. Subscript h, h-1, l and l+1 represent the highest occupied molecular orbital (HOMO), HOMO-1, the lowest unoccupied molecular orbital (LUMO) and LUMO+1 of dG or dC. ^edG and dC represent the intramolecular excited states of deoxyguanosine and deoxycytidine, respectively. ET(s) and ET(h) represent the electron transfer excited states from guanine to cytosine through the stacking and hydrogen-bonding interactions, respectively. ^fExperimental values of Z-DNA.²

Table 9. Excited States of the Rotational Model at $\Delta R = +2.0 \text{ \AA}$ ($\Delta A = 30^\circ$)

state	SAC-CI						exptl.(eV/nm)	
	EE (eV) ^a	EE (nm) ^a	Osc ^b	Rot ^c	nature ^d	type ^e	CD ^f	UV ^f
1 ¹ A	4.69	264	0.106	8.33	$\pi_{c,h} \rightarrow \pi_{c,l}^*$	dC	4.19/296	4.28/290
2 ¹ A	4.76	261	0.109	-28.83	$\pi_{g,h} \rightarrow \pi_{g,l}^*$	dG		4.28/290
3 ¹ A	4.83	256	0.051	151.63	$\pi_{g,h} \rightarrow \pi_{g,l}^*$	dG	4.43/280 (B-DNA)	
4 ¹ A	4.87	254	0.136	-104.05	$\pi_{c,h} \rightarrow \pi_{c,l}^*$	dC		4.28/290
5 ¹ A	5.06	245	0.029	194.04	$\pi_{c,h-1} \rightarrow \pi_{c,l}^*$	dC	4.51/275	
6 ¹ A	5.12	242	0.497	-204.73	$\pi_{c,h-1} \rightarrow \pi_{c,l}^*$	dC		4.84/256
7 ¹ A	5.22	237	0.010	-1.09	$\pi_{g,h} \rightarrow \pi_{c,l}^*$	ET(s)		
8 ¹ A	5.24	236	0.582	81.87	$\pi_{g,h-1} \rightarrow \pi_{g,l}^* + \pi_{g,h} \rightarrow \pi_{c,l}^*$	dG + ET(s)		4.84/256
9 ¹ A	5.25	236	0.074	33.82	$\pi_{g,h} \rightarrow \pi_{c,l}^*$	ET(s)		
10 ¹ A	5.28	235	0.138	-21.01	$\pi_{g,h} \rightarrow \pi_{g,l+1}^*$	dG		4.84/256
11 ¹ A	5.39	230	0.001	-5.22	$n_g \rightarrow \pi_{g,l}^*$	dG		
12 ¹ A	5.48	226	0.004	-0.77	$\pi_{g,h} \rightarrow \pi_{c,l}^*$	ET(h)		
13 ¹ A	5.50	225	0.005	-7.72	$n_c \rightarrow \pi_{c,l}^*$	dC		
14 ¹ A	5.58	222	0.003	-4.49	$n_g \rightarrow \pi_{g,l}^*$	dG		

^aExcitation energy. ^bOscillator strength. ^cRotatory strength (10^{-40} cgs). ^dSubscript g and c represent guanine and cytosine, respectively. Subscript h, h-1, l and l+1 represent the highest occupied molecular orbital (HOMO), HOMO-1, the lowest unoccupied molecular orbital (LUMO) and LUMO+1 of dG or dC. ^edG and dC represent the intramolecular excited states of deoxyguanosine and deoxycytidine, respectively. ET(s) and ET(h) represent the electron transfer excited states from guanine to cytosine through the stacking and hydrogen-bonding interactions, respectively. ^fExperimental values of Z-DNA except for "B-DNA".²

explained in the previous section. The excitation energies, oscillator strengths, rotatory strengths, natures, and type of the excited states obtained from the SAC-CI calculations of the rotational models are shown in Tables 8 and 9.

For the SAC-CI CD spectrum of the rotational model at $\Delta R = \pm 0.0 \text{ \AA}$, the negative peak is calculated to be at lower energy region and its intensity is weaker, as compared with that of the normal model. Because the six-membered ring of the purine base tidily overlaps with the pyrimidine base between the two bases (cytosine and guanine), the excitation energies of the ET excitation (1 and 2¹A) from guanine to cytosine through the stacking interaction are calculated to be at a lower energy region (see Table 8) than those of the X-ray model. However, because the 2¹A excited states has a positive rotatory strength, the negative peak at 295 nm is weak due to the cancellation.

The two positive peaks are calculated to be at the range of 240 to 300 nm. However, the positive peak of the normal model is in the middle of the two positive peaks of the rotational model. Therefore, if we use the larger fwhm value, the two positive peaks would become a single peak and its peak position becomes similar to that of the normal model. On the other hand, the SAC-CI UV spectrum is similar to that of the normal model.

For the SAC-CI CD spectrum of the rotational model at $\Delta R = +2.0 \text{ \AA}$, the negative peak is not calculated in the lower energy region, though its geometrical parameters are the same as the normal model at $\Delta R = +2.0 \text{ \AA}$ with the exception of the angle between the two base pairs. On the other hand, at $\Delta R = +2.0 \text{ \AA}$ the SAC-CI UV spectrum of the rotational model is similar to that of the normal model. However, the shoulder peak of the

rotational model is weaker than that of the normal model. Namely, by the rotation of the base pair, both SAC-CI CD and UV spectra come closer to the feature of the B-DNA than that of the Z-DNA.

Table 9 shows that the lowest excited state is the intramolecular excitation of cytosine, similar to those of the weak stacking models ($\Delta R = +0.6$ to $+2.0$ Å). However, its rotatory strength is positive, opposite to those of the weak stacking models. Therefore, the SAC-CI CD spectrum of the rotational model is positive in the lower energy region. The sum of the oscillator strength of the rotational model is weaker for the lowest four excited states but stronger for the 5 to 10^1 Å excited states than those of the normal model at $\Delta R = +2.0$ Å. Therefore, the SAC-CI UV spectrum of the rotational model at $\Delta R = +2.0$ Å comes closer to the experimental UV spectrum of the B-DNA.

7. CONCLUSION

We have elucidated the relationship between the CD spectra of DNA and the stacking interaction between the two guanine-cytosine pairs by the distance change between the two base pairs of the Z-DNA model. The SAC-CI CD spectrum of the X-ray model agreed with the feature of the experimental CD spectrum of Z-DNA. The two lowest excited states, which are the electron transfer (ET) excitation from guanine to cytosine through the stacking interaction, are the origin of the strong negative peak at 295 nm of the CD spectra of Z-DNA. As the distance between the two base pairs increases, the negative peak at 295 nm is reduced in strength. Instead, the positive peak at 275 nm is increased in strength. Because the stacking interaction become weaker with the increase of the distance between the two base pairs, the stacking ET excited states are calculated to be at a higher energy region and become the origin of the positive peak at 275 nm along with the intramolecular excited states for the $\Delta R = +2.0$ Å model. However, the SAC-CI UV spectral change is small for the distance change between the two base pairs, as compared with the SAC-CI CD spectra. Therefore, the negative peak at 295 nm of the CD spectra of DNA correlates strongly with the stacking interaction between the two base pairs.

We have also elucidated the rotational effect of the CD spectra of DNA by rotating 30° between the two base pairs from the normal models. For the rotation at $\Delta R = \pm 0.0$ Å, the negative peak at 295 nm becomes weak, though the overlap between the two base pairs is large. On the other hand, both of the SAC-CI CD and UV spectra of the rotational model at $\Delta R = +2.0$ Å have the features of the experimental CD and UV spectra of the B-DNA more than those of the normal model at $\Delta R = +2.0$ Å, although the geometrical parameters obtained from the Z-DNA were used except for the distance and the angle between the two base pairs. The present studies revealed that the intensity at 295 nm of CD spectra is an indicator of the stacking interaction of DNA; as the stacking interaction increases, the peak at 295 nm of the CD spectra becomes strongly negative as seen for Z-DNA, while as the stacking interaction becomes weaker the negative peak at 295 nm disappears as seen for B-DNA. The X-ray geometry of the Z-DNA provides a strong negative peak at 295 nm of the CD spectra. However, the intensity of the negative peak is weakened by the distance change as well as the angle change between the two base pairs

■ ASSOCIATED CONTENT

Supporting Information

Coordinate of the X-ray model and the rotational model at $\Delta R = \pm 0.0$ Å. The Supporting Information is available free of charge on the ACS Publications website at DOI: 10.1021/acs.jpca.5b02848.

■ AUTHOR INFORMATION

Corresponding Author

*E-mail: h.nakatsuji@qcri.or.jp. Phone: +81-75-634-3211. Fax: +81-75-634-3211.

Notes

The authors declare no competing financial interest.

■ ACKNOWLEDGMENTS

The computations were performed using the computers at the Research Center for Computational Science, Okazaki, Japan, whom we acknowledge. We also thank the support of Mr. Nobuo Kawakami for the researches of QCRI.

■ REFERENCES

- (1) Rich, A.; Nordheim, A.; Wang, A. H.-J. The Chemistry and Biology of Left-Handed Z-DNA. *Annu. Rev. Biochem.* **1984**, *53*, 791–846.
- (2) Tran-Dinh, S.; Taboury, J.; Neumann, J.-M.; Huynh-Dinh, T.; Genissel, B.; d'Estaintot, B. L.; Igolen, J. ^1H NMR and Circular Dichroism Studies of the B and Z Conformations of the Self-Complementary Deoxyhexanucleotide d(m⁵C-G-C-G-m⁵C-G): Mechanism of the Z-B-Coil Transitions. *Biochemistry* **1984**, *23*, 1362–1371.
- (3) Sugiyama, H.; Kawai, K.; Matsunaga, A.; Fujimoto, K.; Saito, I.; Robinson, H.; Wang, A. H.-J. Synthesis, Structure and Thermodynamic Properties of 8-Methylguanine-Containing Oligonucleotides: Z-DNA under Physiological Salt Conditions. *Nucleic Acids Res.* **1996**, *24*, 1272–1278.
- (4) Kawai, K.; Saito, I.; Sugiyama, H. Conformation Dependent Photochemistry of 5-Halouracil-Containing DNA: Stereospecific 2' α -Hydroxylation of Deoxyribose in Z-form DNA. *J. Am. Chem. Soc.* **1999**, *121*, 1391–1392.
- (5) Oyoshi, T.; Kawai, K.; Sugiyama, H. Efficient C2' α -Hydroxylation of Deoxyribose in Protein-Induced Z-Form DNA. *J. Am. Chem. Soc.* **2003**, *125*, 1526–1531.
- (6) Xu, Y.; Ikeda, R.; Sugiyama, H. 8-Methylguanosine: A Powerful Z-DNA Stabilizer. *J. Am. Chem. Soc.* **2003**, *125*, 13519–13524.
- (7) Tashiro, R.; Sugiyama, H. Biomolecule-Based Switching Devices that Respond Inversely to Thermal Stimuli. *J. Am. Chem. Soc.* **2005**, *127*, 2094–2097.
- (8) *Circular Dichroism: Principles and Applications*; Berova, N., Nakanishi, K., Woody, R. W., Eds; Wiley-VCH: New York, 2000.
- (9) Birke, S. S.; Moses, M.; Kagalovsky, B.; Jano, D.; Gulotta, M.; Diem, M. Infrared CD of Deoxy Oligonucleotides. Conformational Studies of 5'd(GCGC)3', 5'd(CGCG)3', 5'd(CCGG)3', and 5'd(GGCC)3' in Low and High Salt Aqueous Solution. *Biophys. J.* **1993**, *65*, 1262–1271.
- (10) Wang, L.; Keiderling, T. A. Helical Nature of Poly(dl-dC)-Poly(dl-dC). Vibrational Circular Dichroism Results. *Nucleic Acids Res.* **1993**, *21*, 4127–4132.
- (11) Andrushchenko, V.; Wieser, H.; Bour, P. B-Z Conformational Transition of DNA Monitored by Vibrational Circular Dichroism. Ab Initio Interpretation of the Experiment. *J. Phys. Chem. B* **2002**, *106*, 12623–12634.
- (12) Miyahara, T.; Nakatsuji, H.; Sugiyama, H. Helical Structure and Circular Dichroism Spectra of DNA: A Theoretical Study. *J. Phys. Chem. A* **2013**, *117*, 42–55.
- (13) Hobza, P.; Šponer, J. Structure, Energetics, and Dynamics of the Nucleic Acid Base Pairs: Nonempirical *Ab Initio* Calculations. *Chem. Rev.* **1999**, *99*, 3247–3276.

- (14) Šponer, J.; Riley, K. E.; Hobza, P. Nature and Magnitude of Aromatic Stacking of Nucleic Acid Bases. *Phys. Chem. Chem. Phys.* **2008**, *10*, 2595–2610.
- (15) Šponer, J.; Šponer, J. E.; Mládek, A.; Jurečka, P.; Banáš, P.; Otyepka, M. Nature and Magnitude of Aromatic Base Stacking in DNA and RNA: Quantum Chemistry, Molecular Mechanics, and Experiment. *Biopolymers* **2013**, *99*, 978–988.
- (16) Nakatsuji, H.; Hirao, K. Cluster Expansion of the Wavefunction. Symmetry-Adapted-Cluster Expansion, Its Variational Determination, and Extension of Open-Shell Orbital Theory. *J. Chem. Phys.* **1978**, *68*, 2053–2065.
- (17) Nakatsuji, H. Cluster Expansion of the Wavefunction. Excited States. *Chem. Phys. Lett.* **1978**, *59*, 362–364.
- (18) Nakatsuji, H. Cluster Expansion of the Wavefunction. Electron Correlations in Ground and Excited States by SAC (Symmetry-Adapted-Cluster) and SAC-CI Theories. *Chem. Phys. Lett.* **1979**, *67*, 329–333.
- (19) Nakatsuji, H. Cluster Expansion of the Wavefunction. Calculation of Electron Correlations in Ground and Excited States by SAC and SAC-CI Theories. *Chem. Phys. Lett.* **1979**, *67*, 334–342.
- (20) Nakatsuji, H. Electronic Structures of Ground, Excited, Ionized, and Anion States Studied by the SAC/SAC-CI Theory. *Acta Chim. Hung.* **1992**, *129*, 719–776.
- (21) Nakatsuji, H. SAC-CI Method: Theoretical Aspects and Some Recent Topics; In *Computational Chemistry – Reviews of Current Trends*; Leszczynski, J., Ed.; World Scientific: Singapore, 1997; Vol. 2, pp 62–124.
- (22) Nakatsuji, H. Deepening and Extending the Quantum Principles in Chemistry. *Bull. Chem. Soc. Jpn.* **2005**, *78*, 1705–1724.
- (23) Ehara, M.; Hasegawa, J.; Nakatsuji, H. SAC-CI Method Applied to Molecular Spectroscopy. In *Theory and Applications of Computational Chemistry: The First 40 Years, A Volume of Technical and Historical Perspectives*; Dykstra, C. E., Frenking, G., Kim, K. S., Scuseria, G. E., Eds.; Elsevier: Oxford, U.K., 2005; pp 1099–1141.
- (24) Hasegawa, J.; Nakatsuji, H. Exploring Photo-Biology and Biospectroscopy with the SAC-CI (Symmetry-Adapted Cluster-Configuration Interaction) Method. In *Radiation Induced Molecular Phenomena in Nucleic Acid: A Comprehensive Theoretical and Experimental Analysis*; Shukla, M. Leszczynski, J., Eds.; Springer: New York, 2008; Chapter 4, pp 93–124.
- (25) Miyahara, T.; Nakatsuji, H. Conformational Dependence of the Circular Dichroism Spectra of α -Hydroxyphenylacetic Acid: A ChiraSac study. *J. Phys. Chem. A* **2013**, *117*, 14065–14074.
- (26) Miyahara, T.; Nakatsuji, H.; Wada, T. Circular Dichroism Spectra of Uridine Derivatives: ChiraSac Study. *J. Phys. Chem. A* **2014**, *118*, 2931–2941.
- (27) Frisch, M. J.; Trucks, G. W.; Schlegel, H. B.; Scuseria, G. E.; Robb, M. A.; Cheeseman, J. R.; Scalmani, G.; Barone, V.; Mennucci, B.; Petersson, G. A.; Nakatsuji, H.; Caricato, M.; Li, X.; Hratchian, H. P.; Izmaylov, A. F.; Bloino, J.; Zheng, G.; Sonnenberg, J. L.; Hada, M.; Ehara, M.; Toyota, K.; Fukuda, R.; Hasegawa, J.; Ishida, M.; Nakajima, T.; Honda, Y.; Kitao, O.; Nakai, H.; Vreven, T.; Montgomery, J. A., Jr.; Peralta, P. E.; Ogliaro, F.; Bearpark, M.; Heyd, J. J.; Brothers, E.; Kudin, K. N.; Staroverov, V. N.; Kobayashi, R.; Normand, J.; Raghavachari, K.; Rendell, A.; Burant, J. C.; Iyengar, S. S.; Tomasi, J.; Cossi, M.; Rega, N.; Millam, N. J.; Klene, M.; Knox, J. E.; Cross, J. B.; Bakken, V.; Adamo, C.; Jaramillo, J.; Gomperts, R.; Stratmann, R. E.; Yazyev, O.; Austin, A. J.; Cammi, R.; Pomelli, C.; Ochterski, J. W.; Martin, R. L.; Morokuma, K.; Zakrzewski, V. G.; Voth, G. A.; Salvador, P.; Dannenberg, J. J.; Dapprich, S.; Daniels, A. D.; Farkas, Ö.; Ortiz, J. V.; Cioslowski, J.; Fox, D. J. *Gaussian 09*, Revision B.01; Gaussian, Inc.: Wallingford, CT, 2009.
- (28) Bousquet, D.; Fukuda, R.; Maitarad, P.; Jacquemin, D.; Ciofini, I.; Adamo, C.; Ehara, M. Excited-State Geometries of Heteroaromatic Compounds: A Comparative TD-DFT and SAC-CI Study. *J. Chem. Theory Comput.* **2013**, *9*, 2368–2379.
- (29) Ehara, M.; Fukuda, R.; Adamo, C.; Ciofini, I. Chemically Intuitive Indices for Charge-Transfer Excitation Based on SAC-CI and TD-DFT Calculations. *J. Comput. Chem.* **2013**, *34*, 2498–2501.
- (30) Leang, S. S.; Zahariev, F.; Gordon, M. S. Benchmarking the Performance of Time-Dependent Density Functional Methods. *J. Chem. Phys.* **2012**, *136*, 104101–1–12.
- (31) Dunning, T. H., Jr.; Hay, P. J. In *Methods of Electronic Structure Theory (Modern Theoretical Chemistry)*; Schaefer, H. F., III., Ed.; Plenum: New York, 1977; Vol. 3, pp 1–27.
- (32) Nakatsuji, H. Cluster Expansion of the Wavefunction. Valence and Rydberg Excitations, Ionizations, and Inner-Valence Ionizations of CO₂ and N₂O Studied by the SAC and SAC-CI Theories. *Chem. Phys.* **1983**, *75*, 425–441.